Int. J. Electrochem. Sci., 14 **(2019)** 8326 – 8339, doi: 10.20964/2019.08.117

International Journal of ELECTROCHEMICAL SCIENCE
www.electrochemsci.org

Poly(*o*-phenylenediamine)-Multiwalled Carbon Nanotube Nanocomposite Based Electrochemical Sensing Platform for Paraquat Detection

Tharini Jeyapragasam[1,], Ramachandran Raju[2], Shen-Ming Chen[3,*], Ramiah Saraswathi[4], Ashraf A. Hatamleh[5], Tse-Wei Chen[3,6], Syang-Peng Rwei[6,7]*

[1] Sethu Institute of Technology, Pulloor-626115, Kariapatti, TN, India
[2] Madura College, Department of Chemistry, Madurai- 625021, TN, India
[3] Department of Chemical Engineering and Biotechnology, National Taipei University of Technology, Taipei 106, Taiwan, ROC.
[4] Department of Materials Science, School of Chemistry, Madurai Kamaraj University, Madurai - 625 021, Tamilnadu, India
[5]Department of Botany and Microbiology, College of Science, King Saud University, P.O. Box 2455, Riyadh 11451, Saudi Arabia.
[6]Research and Development Center for Smart Textile Technology, National Taipei University of Technology, Taipei 106, Taiwan, ROC
[7] Institute of Organic and Polymeric Materials, National Taipei University of Technology, Taipei 106, Taiwan, ROC
[*]E-mail: smchen78@ms15.hinet.net (Shen-Ming Chen), tharinichem@gmail.com (J.Tharini)

Received: 5 May 2019 / *Accepted:* 15 June 2019 / *Published:* 30 June 2019

Poly(o-phenylenediamine)-Multiwalled Carbon Nanotube nanocomposite was prepared by the electropolymerization of o-phenylenediamine (PoPD) onto the functionalized multiwalled carbon nanotube nanocomposite (MWCNT) which acts as the good sensing materials for the electrochemical sensing of paraquat. Atomic force microscopy (AFM) image confirms somewhat large agglomerated structures suggesting the deposition of PoPD onto the MWCNT. The electrochemical reduction of paraquat at four electrodes viz. glassy carbon electrode (GCE), MWCNT/GCE, PoPD/GCE and PoPD-MWCNT/GCE are studied. The cyclic voltammograms has been studied for the electrochemical reduction of paraquat at four different electrodes such as glassy carbon electrode (GCE), MWCNT/GCE, PoPD/GCE and PoPD-MWCNT/GCE. Poly (o-phenylenediamine)-Multiwalled Carbon Nanotube nanocomposite shows highest cathodic current compared to other modified eletrodes. Different experimental parameters such as influence of scan rate and pH have been optimized for the sensor studies. The sensor calibration plot for paraquat has been constructed using square wave voltammetry (SWV) sensor in the linear range from 8.8×10^{-7} M to 2.5×10^{-8} M. The developed sensor resulted in a detection limit and current sensitivity values of 1.4×10^{-9} M and 80.38 μA μM^{-1} respectively. Real sample analysis for cabbage samples and interference studies in the presence of selected metal ions and surfactants have been carried out.

Keywords: Paraquat, Square wave voltammetry, multiwalled carbon nanotube nanocomposite, o-Phenylenediamine

1. INTRODUCTION

Paraquat, also known as methyl viologen (1, 1'-Dimethyl-4, 4'-bipyridinium dichloride) is the most popular herbicide in the world [1] which finds extensive application in the weed control in plantation crops and fruit orchards. It is used as the desiccant for pineapples, sugarcane, soybeans, and sunflower. It is highly toxic and has been classified under Level I - extremely hazardous pesticides with a lethal dose of 35 mg/kg [2]. The herbicidal properties, toxicology and analytical determination of the bipyridinium herbicides can be found in an excellent review [3]. A number of analytical methods have been used for the sensing of paraquat in water, agricultural products, and biological fluids. Among them, spectrophotometry [4] and chromatography [5,6] are the most commonly used analytical methods. These conventional methods, however, require extensive sample pretreatment to enhance the analytical sensitivity. Electrochemical methods have emerged as a suitable, straightforward and reliable analytical procedure for the sensing of paraquat.

The herbicidal properties of paraquat were first described in 1958 and introduced commercially in 1962 [1]. Engelhardt and Mckinley [7] reported the normal polarographic determination of paraquat in 0.1 M KCl with 2×10^{-6} M as the possible limit of detection. The redox property of paraquat makes voltammetry as the suitable technique for its determination. For example, carbon paste electrode chemically modified with amberlite XAD-2 resin [8], sodium form of zeolite-Y [9] were found to improve the selectivity and sensitivity of the voltammetric determination of paraquat. A novel attempt to combine Nafion with different types of clays as a chemical modifier was reported. The enhanced cation exchangeability of the composite combined with the mechanical stability of nafion aids in the determination of trace amount of paraquat in real samples [10]. A multipulse square wave voltammetry on gold microelectrode was established for determining paraquat in natural water, food, and beverage. Paraquat sensor based on microelectrodes was developed without any pretreatment and extraction procedure [12, 13]. A pyrolytic graphite electrode modified with cobalt phthalocyanine was shown to detect paraquat in the concentration range of 5×10^{-7} M to 2.5×10^{-9} M using square wave voltammetry [14]. Mohammed developed paraquat sensor at natural phosphate modified carbon paste electrode using square wave voltammetry (SWV) [15] and carbon paste modified with fluoroapatite [16]. The application of deoxyribonucleic acid (DNA) modified gold nanoparticle immobilized at the gold electrode for the biosensing of paraquat was demonstrated with a detection limit of 1.9×10^{-6} M [17]. In another related study, DNA was electrochemically deposited on a carbon ionic liquid electrode to give a biosensor with a detection limit of 3.6×10^{-6} M [18]. Differential pulse voltammetric detection of paraquat at a bismuth film electrodeposited on a copper substrate was reported. The limit of detection was found to be 9.8×10^{-8} M and the sensor was applied for real sample analysis [19]. Recently, natural and alkali treated sawdust was used to prepare thin film electrodes with good mechanical and wide electrochemical potential range. The sawdust modified electrode presented a good capacity to accumulate paraquat and hence applied to its determination to the nanomolar concentration of paraquat [20]. A composite electrode based on Cu_2O/polyvinylpyrrolidone-graphene modified glassy carbon-rotating disk electrode

has been reported to be capable of sensing paraquat by differential pulse voltammetry [21]. Abdelfettah developed metallic silver nanoparticle electrodeposited on carbon paste electrode for the sensing of paraquat in citric fruit cultures. The linear calibration curve was constructed using SWV with the detection limit of 20 nM with good sensitivity and repeatability [22]. There have been a couple of literatures on the use of polymer modified electrodes for the sensing of paraquat [23, 24].

We report the electrodeposition of o-phenylenediamine (PoPD) onto the multiwalled carbon nanotube (MWCNT) modified glassy carbon electrode. The formed PoPD-MWCNT nanocomposite serves as the effective matrix for the electrochemical detection of paraquat. The excellent mechanical strength of multiwalled carbon nanotube and well-defined redox properties of Poly (o-phenylenediamine) make it as the good sensing materials for paraquat in the nanomolar concentration.

2. EXPERIMENTAL

2.1. Chemicals

Multiwall carbon nanotubes (MWCNT) (diameter 10-15 nm, length 0.1-10 □m), *o*-phenylenediamine (S.D's) were purchased from Sigma-Aldrich. Sodium sulfate (SRL), sulfuric acid, acetic acid, sodium acetate, dipotassium hydrogen phosphate, potassium hydrogen phosphate (Merck) and sodium hydroxide (Qualigens) were used as received.

2.2. Instruments

Electrochemical measurements were performed on an electrochemical workstation (CH Instruments, USA, and Model 680). A one-compartment cell with provision for three electrodes comprising glassy carbon electrode (GCE, 0.07 cm^2) as the working electrode, saturated calomel electrode (SCE) as the reference and large platinum foil electrode as the counter electrode was used. Atomic force microscopy (AFM) images were obtained using an Advanced Physics and Engineering Research instrument (Model A100 SGS).

2.3. Preparation of Functionalized MWCNT

The commercial MWCNT sample was functionalized by a simple acid treatment procedure to introduce hydrophilic functional groups. A chemical oxidation treatment of MWCNT was carried out with the mixture of concentrated nitric acid and sulphuric acid [2]. 50 mg of MWCNT was added to 24 mL of the acid mixture and refluxed for 5 h (Scheme 1). It is cooled and the mixture was washed with plenty of double distilled water until the washings showed no acidity. The acid functionalized MWCNT could be dispersed in aqueous solution by sonication due to the presence of hydrophilic functional groups such as acid and hydroxy group. The dispersions were quite stable for several weeks and could be stored and reused.

Scheme 1. Functionalization of MWCNT using simple acid treatment procedure.

2.4. Preparation of MWCNT Modified GCE (MWCNT/GCE)

1 mg of functionalized MWCNT is dispersed in 1 mL of double distilled water by sonication. About 5 □L of the dispersion is casted on the GCE and then dried in the room temperature to obtain MWCNT/GCE.

2.5. Preparation of Poly(o-phenylenediamine) modified GCE (PoPD/GCE) and Poly(o-phenylenediamine)-MWCNT Nanocomposite Modified GCE (PoPD-MWCNT/GCE)

The P*o*PD/GCE was obtained by electrodeposition of the 5 x 10^{-4} M *o*-phenylenediamine in 0.2 M Na_2SO_4 at pH 1 in the potential range from -300 mV to 1000 mV as already reported in the literature [26]. The P*o*PD-MWCNT/GCE was prepared following a similar procedure as described above except that the polymer was electrodeposited on the MWCNT/GCE. Scheme 2 pictorially represents the coating of PoPD-MWCNT onto the GCE. The formation of PoPD-MWCNT nanocomposite is already is characterized in our previous reports [26].

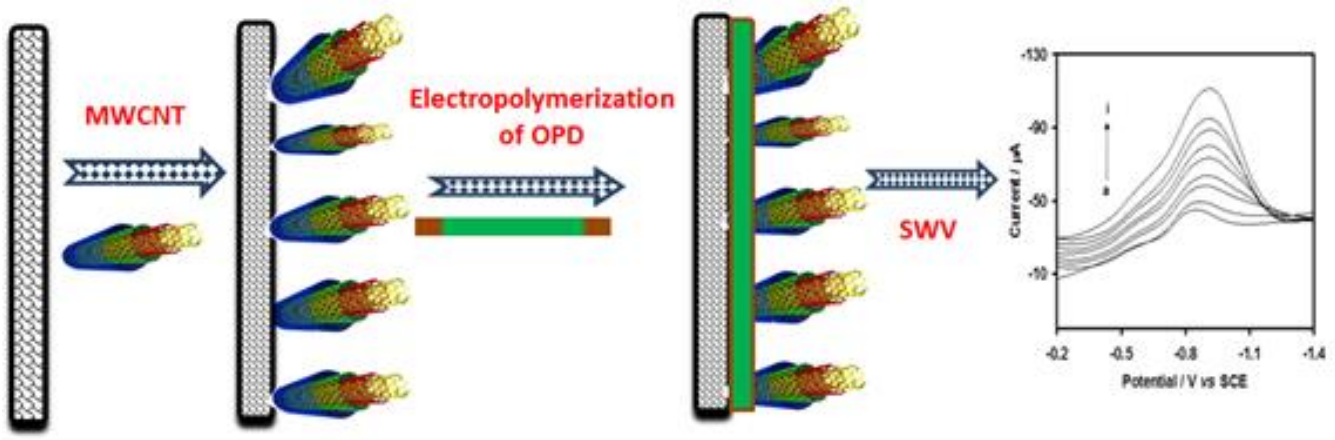

Scheme 2. Schematic representation of coating of P*o*PD-MWCNT onto the GCE.

3. RESULTS AND DISCUSSION

3.1. Electrocatalysis of Paraquat at PoPD-MWCNT/GCE

Fig. 1 A shows the cyclic voltammograms at GCE in the presence and absence of paraquat at 0.01V s^{-1} in the derated condition. The cyclic voltammogram for the reduction of paraquat shows two redox processes at E_{pc1} = - 0.71 V, E_{pa1} = -0.64 V, E_{pc2} = -1.05 V and E_{pa2} = -0.98 V which is due to the reduction of paraquat dication into paraquat cation radical. The two redox couples are highly reversible corresponding to the transfer of one electron in each step (Eq. 1 and 2). In the anodic process, a poorly defined peak is observed at about -0.9 V due to the electrode reaction is given in (Eq. 3)

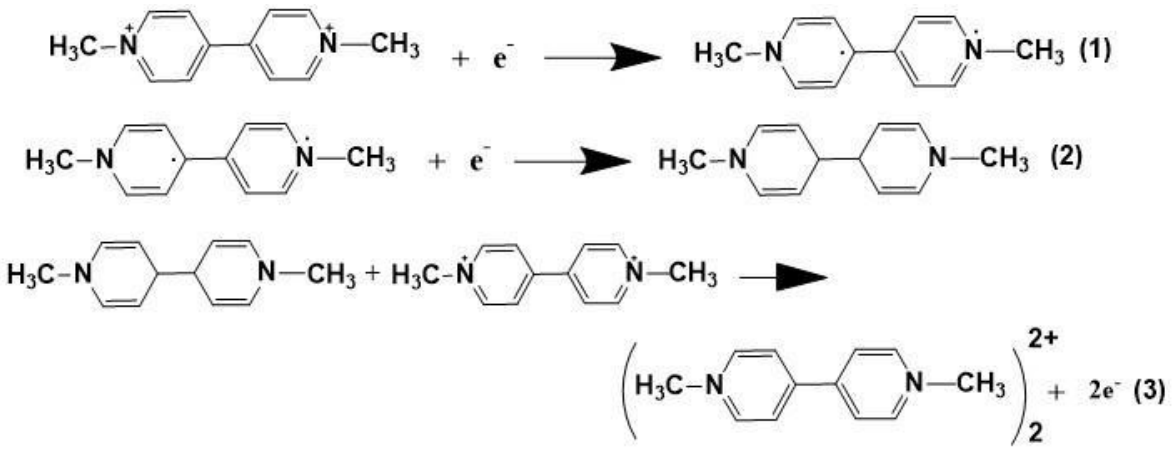

Figure 1. B shows the cyclic voltammograms at MWCNT/GCE in the presence and absence of paraquat at 0.01V $s^{-1.}$ The large background current of MWCNT/GCE can be attributed to the capacitive current contribution by the MWCNT present on the electrode surface [26].

The cyclic voltammogram for the reduction of paraquat at MWCNT/GCE at 0.01 V s^{-1} (Fig. 1B) also shows two redox processes (E_{pc1} = - 0.69 V, E_{pa1} = -0.65 V, E_{pc2} = - 1.0 V and E_{pa2} = -0.91 V) as observed in the case of GCE. The voltammetric behaviour is similar to that reported in literature [27-30].

Fig. 1C (a), 1D (a) shows the cyclic voltammograms at P*o*PD/GCE and PoPD-MWCNT/GCE in the absence of paraquat at 0.01V $s^{-1.}$ At both the electrodes, presence of redox couple (P*o*PD/GCE, E_{pc} = -0.75V, E_{pa} = -0.57 V; P*o*PD-MWCNT/GCE, E_{pc} = -0.91 V, E_{pa} = -0.6 V) confirms the redox reaction of the polymer. The cathodic peak current at the PoPD-MWCNT/GCE is about three times higher than P*o*PD/GCE.

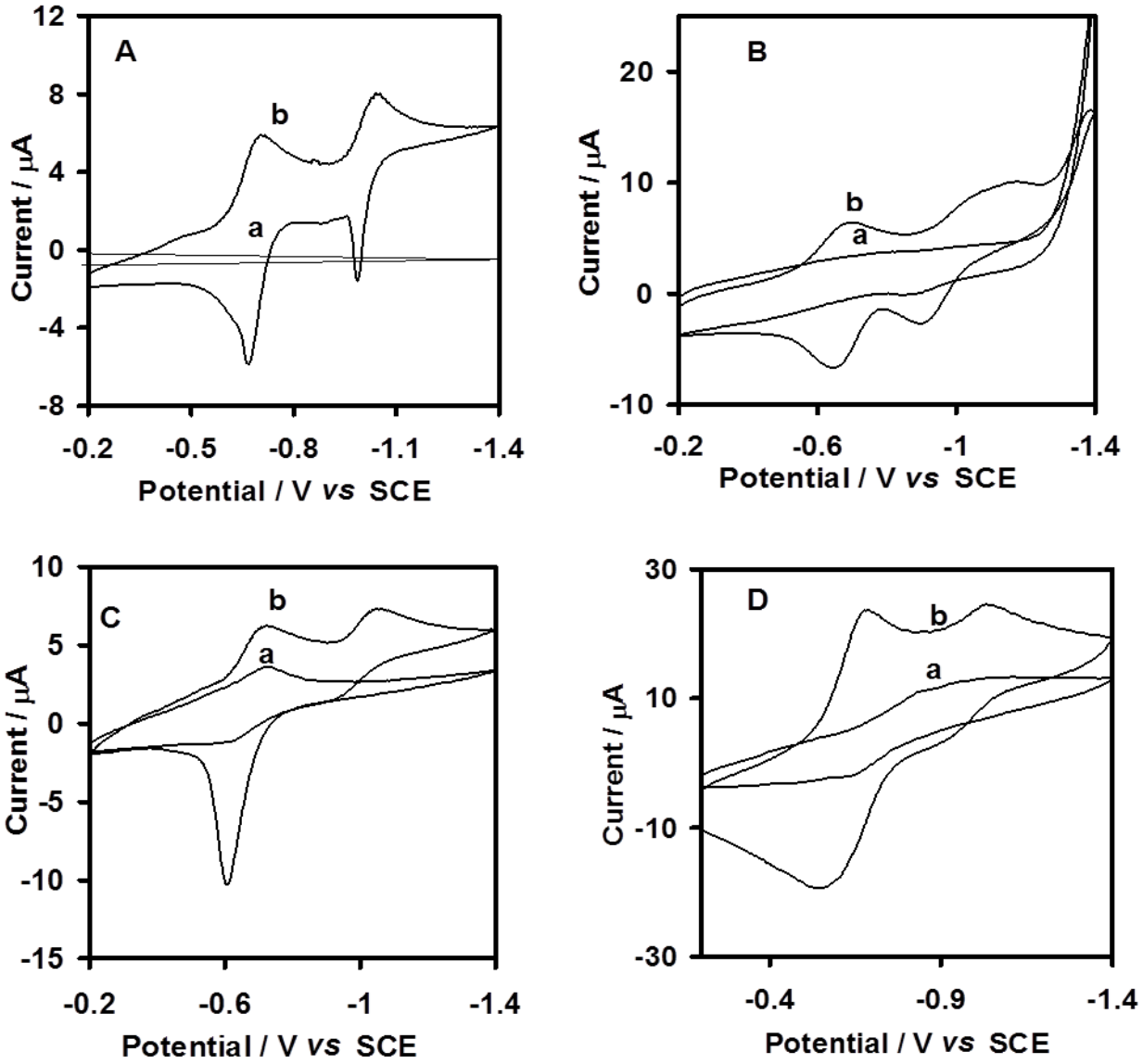

Figure 1 Cyclic voltammograms in 0.1 M PBS (pH 9.8) at (A) GCE (B) MWCNT/GCE (C) P*o*PD/GCE (D) P*o*PD-MWCNT/GCE. (a) in the absence and (b) in the presence of 4×10^{-3}M paraquat. Scan rate = 0.01 V s^{-1}.

Fig. 1C (b), 1D (b) shows the cyclic voltammograms at P*o*PD/GCE and PoPD-MWCNT/GCE in the presence of paraquat at 0.01V $s^{-1.}$ It shows two cathodic peaks and one anodic peak (E_{pc1} = - 0.74 V, E_{pa1} = -0.52 V, E_{pc2} = - 1.04 V at P*o*PD/GCE; E_{pc1} = - 0.69 V, E_{pa1} = -0.54 V, E_{pc2} = - 1.04 V at PoPD-MWCNT/GCE) corresponding to the first process are observed. The anodic peak corresponding to the second cathodic process (E_{pa2} = -0.9 V) could be observed only at very high sweep rates at both the electrodes. The electrochemical reduction of paraquat has been studied for the GCE, MWCNT/GCE, P*o*PD/GCE and P*o*PD-MWCNT/GCE at different sweep rates (0.005 to 0.2 V s^{-1}) in PBS (pH 9.8) (Fig. 2). The insert in Fig. 2 shows representative I_{pc1}-$v^{1/2}$ linear plots at the respective electrode. A detailed analysis of peak current values against the scan rate shows a linear correlation which confirms the diffusion-controlled process. Paraquat can exist in three redox states (Eq. 1)

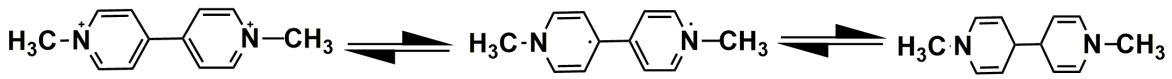

--------(1)

The first reduction step is highly reversible and can be cycled many times without significant side reaction. Further reduction to the fully reduced state is less reversible due to the insolubility of MV^0 molecules (Scheme 3) [27-30]. Table 1 presents the voltammetric data at 0.01 Vs^{-1} for the reduction of paraquat at the four electrodes investigated. It is observed that the reduction and oxidation peak potentials at the four electrodes are nearly the same at all electrodes. But the magnitude of peak current depends on the nature of modified electrode.

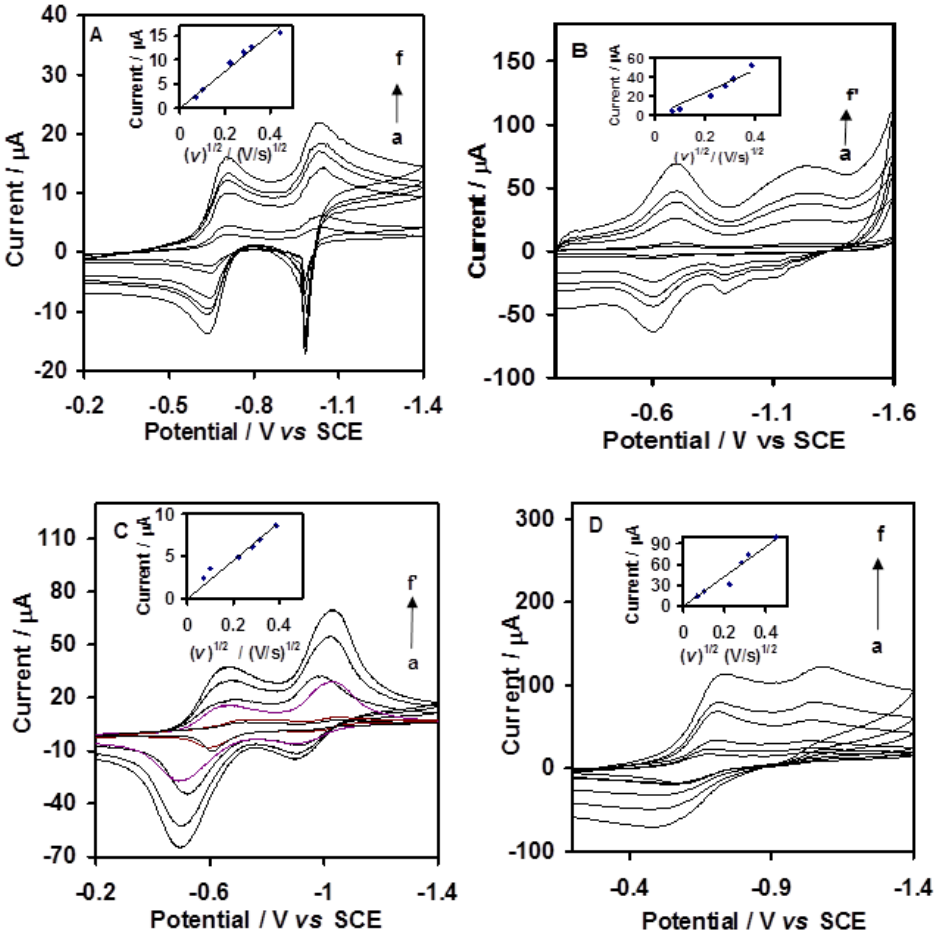

Figure 2. Cyclic voltammograms in 0.1 M PBS (pH 9.8) containing 4×10^{-3} M paraquat (A) GCE (B) MWCNT/GCE (C) P*o*PD/GCE (D) PoPD-MWCNT/GCE at various scan rates (a) 0.005 V s^{-1} (b) 0.01 V s^{-1} (c) 0.05 V s^{-1} (d) 0.08 V s^{-1} (e) 0.1 V s^{-1} (f) 0.2 V s^{-1} (f') 0.15 V s^{-1}

The cyclic voltammetric data at the four electrodes were compared which shows the highest current at the PoPD-MWCNT/GCE. This can be attributed to the good synergy between the P*o*PD and MWCNT. It is interesting to note that the I_{pc1} is maximum at P*o*PD-MWCNT/GCE which is nearly four

times larger than that at bare GCE. Therefore it can be expected that the PoPD-MWCNT/GCE can exhibit a maximum sensitivity for the detection of paraquat and hence all further sensor optimization and calibration experiments have been carried out with respect to the first cathodic process at PoPD-MWCNT/GCE.

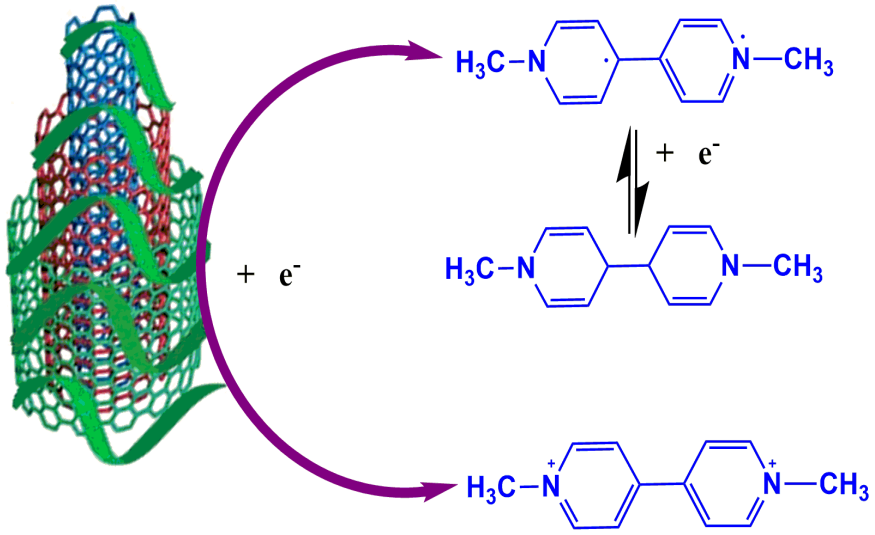

Scheme 3. Schematic representation of reduction paraquat onto the PoPD-MWCNT onto the GCE.

Table 1. Cyclic voltammetric data for the reduction of paraquat at GCE, MWCNT/GCE, PoPD/GCE, PoPD-MWCNT/GCE, Scan rate = 0.01 V s^{-1}.

Electrode	E_{pc1} (V)	E_{pc2} (V)	E_{pa1} (V)	E_{pa2} (V)	I_{pc1} (□A)	I_{pc2} (□A)	I_{pa1} (□A)	I_{pa2} (□A)
GCE	-0.71	-1.05	-0.64	-0.98	5.49	3.50	4.46	3.30
MWCNT/GCE	-0.69	-1.00	-0.65	-0.91	5.97	4.70	4.88	0.49
PoPD/GCE	-0.74	-1.04	-0.52	-----	2.6	2.03	9.96	----
POPD-MWCNT/GCE	-0.69	-1.04	-0.54	-----	20.10	4.20	19.12	-----

3.2. Optimization of Electrolyte pH

In order to find the maximum sensitivity for the sensing of paraquat at PoPD-MWCNT/GCE, the cyclic voltammograms were recorded in 0.1 M PBS of pH 6.45, 7.45, 8.06 & 9.8. As the pH is increased from 6.45 to 9.8, first cathodic reduction peak increases (20 □A) and reaches the maximum at 9.8. In other words, the absolute cathodic peak current value is observed to be the highest at pH 9.8 (Fig. 3). Therefore further calibration experiments have been carried in PBS (pH 9.8). The cathodic peak potential of paraquat does not with the peak potential because paraquat does not involve the protonation of hydrogen in the rate-determining step.

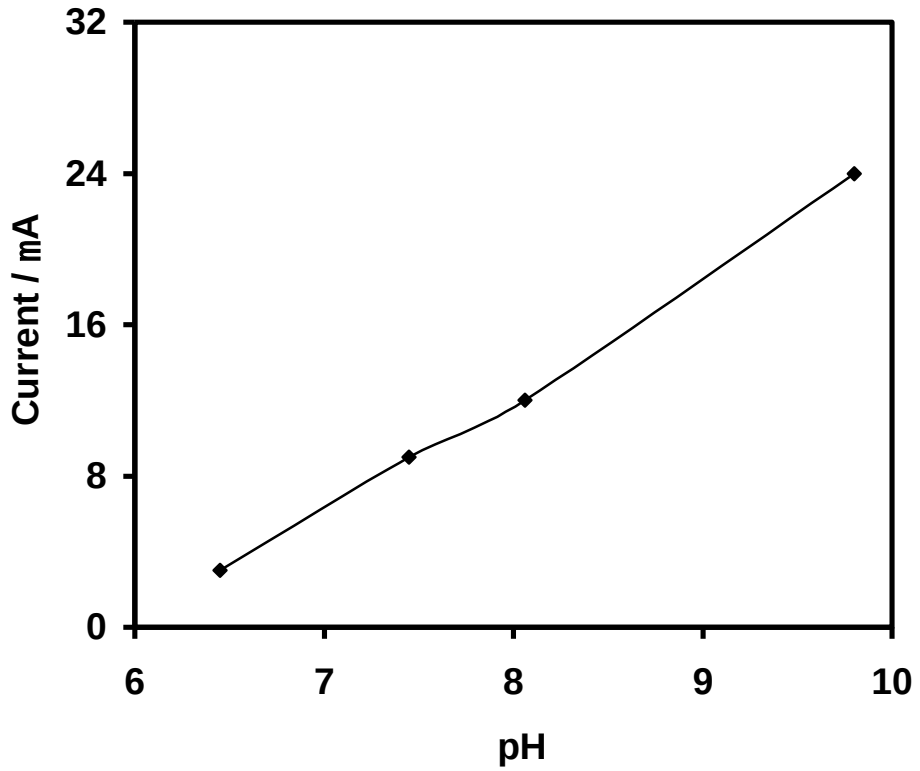

Figure 3. Plot of pH versus first cathodic current at PoPD-MWCNT/GCE.

3.3. Square Wave Voltammetry

In order to find the detection limit of paraquat at the P*o*PD-MWCNT/GCE, a more sensitive technique than cyclic voltammetry needs to be employed. Square wave voltammetry (SWV) has been popular and valuable method in electrochemical sensor applications**.** It offers excellent sensitivity due to the rejection of background currents [31]. In the present work, the SWV experiments have been performed at P*o*PD- MWCNT/GCE in the potential range from -0.3 to -1.4 V at a frequency of 15 Hz and pulse amplitude of 0.025 V in PBS (pH 9.8). Fig. 4 A shows the SWVs of paraquat in the concentration range from 8.8×10^{-7} M to 2.5×10^{-8} M. There is a nearly 0.05 V potential shift to the negative side with increasing analyte concentration. The cathodic current is found to be linear in the entire concentration range with the slope and regression coefficient values of 80.38 □A / □M and 0.99, respectively.

The detection limit can be calculated using Eq. 3 [33].

$$Detection\ Limit = \frac{3 \times S}{N} \quad (2)$$

S = standard deviation of mean current measured at the lowest analyte and N = slope of the calibration plot. In this study, the mean value and standard deviation are calculated to be 0.166 and 0.038 respectively. Using the equation 3, the detection limit and current sensitivity of paraquat are estimated to be 1.4×10^{-9} M and 80.38 □A □M^{-1} respectively for a signal-to-noise of 4.3. The detection limit

observed in the present study is compared to the values [17,18,21,23,24] reported in the literature for various polymer and nanomaterial modified electrodes. (Table. 2). From the tabulated data, it is observed that the detection limit for paraquat at the PoPD-MWCNT is the lowest among the reported values for polymer and nanocomposite modified electrodes. However, it may be notified here that compared to the present work, slightly lower detection limits have been reported non-nano chemically modified electrodes based on carbon paste/Amberlite XAD-2 resin (3.8×10^{-10} M) [8] and natural phosphate modified carbon paste electrode (7.8×10^{-10} M) [15].

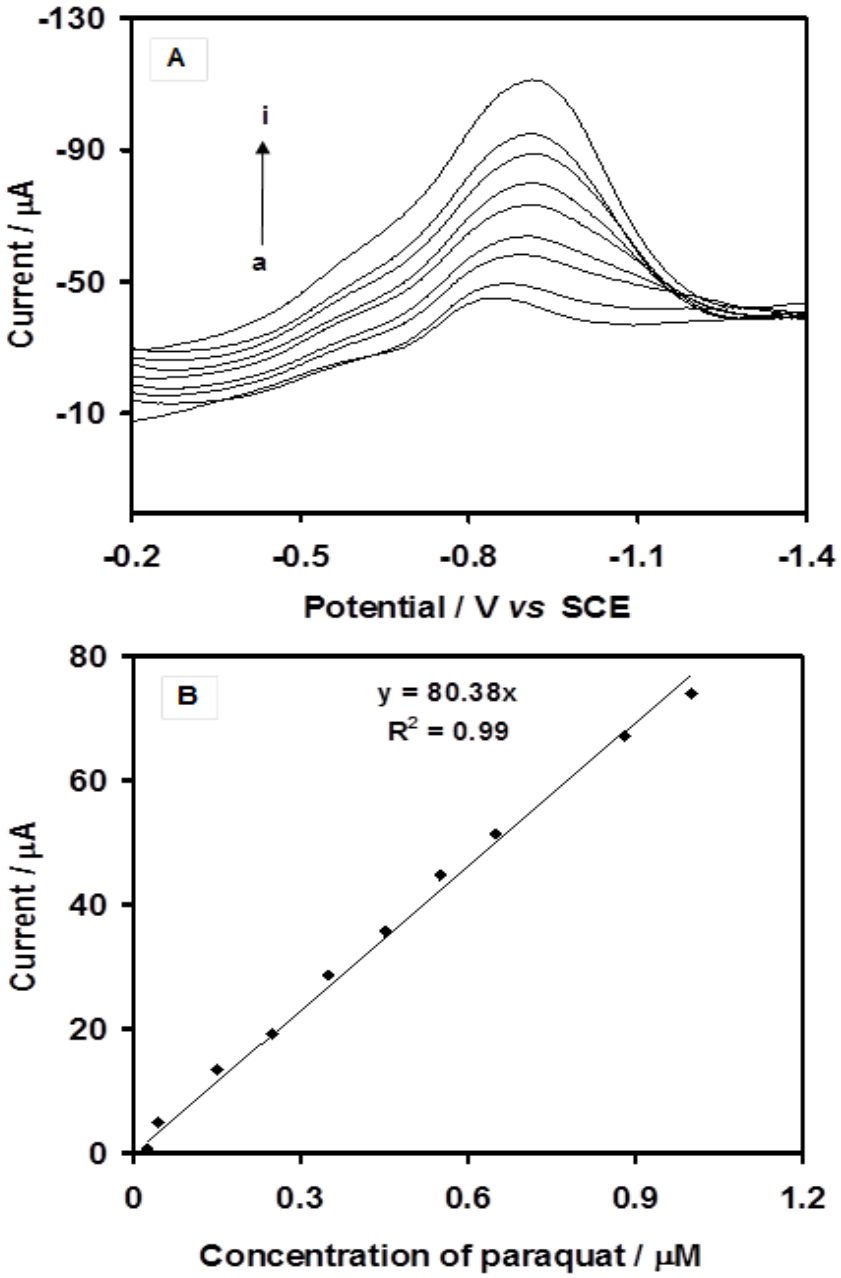

Figure 4. (A) Square wave voltammograms at PoPD-MWCNT/GCE in 0.1M PBS at pH (9.8) at different concentrations of paraquat. in □M a) 0.025 b) 0.045 c) 0.15 d) 0.25 e) 0.35 f) 0.45 g) 0.55 h) 0.65 i) 0.88 B) Sensor calibration plot for paraquat detection.

Table 2. Reported calibration data for paraquat sensor using polymer and nanomaterials modified electrode

Type of Electrode	Method	Linear range (□M)	Detection limit (□M)	Ref
Polyviologen modified gold/quartz	EQCM	0 – 1200	100	24
Poly(*o*-ethoxyaniline)	Impedance	15.5- 38.88	14	23
Copper oxide/polyvinyl pyrrolidine/graphene	DPV	1 – 200	0.26	21
DNA/ Gold nanoparticle	DPV & SWV	5 – 1000	1.3	17
DNA/Carbon ionic liquid	DPV	0.05 – 0.7	0.0036	18
Ag/NP-CPE	SWV	0.1-1000	0.00001	34
CPME	DPAdSV	0.03-1	0.0075	35
Ag-CPE	SWV	0.1-1000	.02	36
PoPD-MWCNT/GCE	SWV	0.025-0.88	0.0001	Present work

EQCM: Quartz crystal microbalance; DPV: Differential pulse voltammetry; SWV: Square wave voltammtry; BR: Brittson Robinson buffer; Ag/NP-CPE: silver /natural phosphate –carbon paste electrode, DPAdSV-Differential Pulse Adsorptive Stripping Voltammetry, CPME- carbon paste electrode modified with biochar

3.4. Interference Studies

Paraquat is likely to be found in the groundwater along with other pesticides, metal, surfactant and clay contaminants. Hence it is necessary to study the inference effects in the detection of paraquat for the real-time use of the developed electrochemical sensor. In the present work, the interference effects of paraquat with heavy metals and surfactants have been investigated by SWV. Copper, cadmium, *N*-cetyl, *N*, *N', N''*-trimethyl ammonium bromide (CTAB) and sodium dodecyl sulphate (SDS) were selected for the interference studies. For a concentration of 1.5×10^{-7} M paraquat, an equal concentration of interfering species was added. The % variation in the SWV peak current of paraquat was determined using Eq. 4.

Percent variation in $I_{pc}(MV) = [I_{pc}(\text{interfering ions}) - I_{pc}(MV)]/ I_{pc}(MV)$ (4)

where I_{pc} (interfering ions) is the square wave voltammetric peak current of the interfering species and $I_{pc}(MV)$ is the cathodic peak current of paraquat. Table 3 shows the interference effect of paraquat in the presence of the different interfering species. Copper and cadmium are found to interfere by increasing the paraquat signal to nearly 5 % whereas CTAB and SDS are found to be interfering by decreasing the paraquat signal intensity by about 4 %.

Table 3. Effect of interfering species on the detection of paraquat at PoPD- MWCNT/GCE.

Ions	% variation in the cathodic peak [i_{pc1}(paraquat) = 100%]
Cu (II)	4.9
Cd(II)	5.3
SDS	-3.9
CTAB	-4.4

3.5. Real Sample Analysis

The developed P*o*PD-MWCNT/GCE has been tested with two vegetable (cabbage) samples. Vegetable sample (cabbage) was purchased from the vegetable vendors and washed with plenty of distilled water. Then 5g of cabbages were spiked with known concentrations of parquat. Then the sample were allowed to stand for 24hours and finally extracted with 30 mL of ether. The supernatants were then filtered through a 0.45 □m membrane and then evaporated to dryness. About 2 mL of ethanol was added to the dry residue and diluted to 100 mL with 0.1M PSB (pH9.8) [37]. The two samples prepared were analyzed using SWV at PoPD-MWCNT in 0.1 M PB (9.8). Table 4, it is confirmed that the P*o*PD-MWCNT/GCE shows good recovery percentage.

Table 4. Recovery data of paraquat present in two cabbage samples at PoPD-MWCNT.

Sample	Added (□M)	Found (□M)	Recovery %
1	0.30	0.25	83
2	0.17	0.15	87

4. CONCLUSION

An electrochemical sensor for the sensing of paraquat has been developed at PoPD-MWCNT/GCE. The nanocomposite shows better electrochemical detection towards paraquat compared to GCE, MWCNT/GCE, P*o*PD/GCE. A highly enhanced electrocatalytic effect at the P*o*DP-MWCNT nanocomposite is observed. The nanocomposite based sensor shows detection limit and sensitivity as 1.4×10^{-9} M and 80 □A □M^{-1} respectively for the paraquat.

ACKNOWLEDGEMENTS
This project was supported by King Saud University, Deanship of Scientific Research, College of Science, Research Center. The authors are grateful for financial support (MOST 107-2113-M-027-005-MY3) from the Ministry of Science and Technology (MOST) and Ministry of Education, Taiwan. We take this opportunity to thank all of the co-workers of in our research groups who have contributed the collecting of research articles and also the author would like to thank Science & Engineering Research Board (SERB), under the grant no. SERB/F/8355/2016-17 dated 16th February 2017, India

References

1. P. Smith and D.Heath, *CRC Crit Rev Toxicol*., 4 (1976) 411.
2. J.F. Dasta, *Am. J. Hosp.,* 35 (1978) 1368.
3. A. Calderbank, *Adv. Pest. Control. Res*., 8 (1968) 127.
4. M.K. Rai, J.V. Das and V.K. Gupta, *Talanta* 45 (1997) 343.
5. R.M.D.Almeida and M. Yonamine, J. Chromatogr B., 87 (2010) 2548.
6. V.A. Simon and A.J. Taylor, *Chromatogr A.,* 153 (1989) 479.
7. J. Engelhardt and W. P. Mckindley, *J. Agri. Food. Chem.,* 4 (1966) 377.
8. E. Alvarez, M. T. Sevilla, J.M. Pinilla and L. Hernandez, *Anal.Chim.Acta.,* 19 (1992) 260.
9. A. Walcarius, L. Lamberts and G. Derouane, *Electrochim. Acta.,* 38 (1993) 2257
10. T. H. Lu and I.W. Sun, *Talanta* 53 (2000) 443
11. J. M. Zen, S.H. Jeng and H. J. Chen, *Anal Chem*., 68 (1996) 498.
12. D. De Souza, S.A.S. Machado, and R.C. Pires, R.C., *Talanta* 69 (2006)1200.
13. D. De Souza and S.A.S. Machado, *Anal.Chim.Acta.* 85(2005) 546
14. I.C.Lopes , D. De Souza, S.A.S. Machado, and A.A.Tanaka, *Anal. Bioanal. Chem.* 388*(* 2007) 1907.
15. M.A. El Mhammedi, Bakasse, and A. Chtaini, *J. Hazard. Mater.* 1(2007)145.
16. M.A. El Mhammedi, M. Bakasse, R. Bachirat, and A. Chtaini, *Food chem.* 110 (2008) 1001.
17. J.A. Ribeiro, C.A. Carreira, C.A., Lee, H.J., Silva, F., Martins, A., and Pereira, C.M., *Electrochim. Acta* **55** (2010) 7892.
18. N. Mai, X. Liu, W. Wei, S. Luo, and W.Liu, *Microchim. Acta* 8 (2011) 174.
19. L. C. S. D. F. Filho, V.B.D. Santos, B.C. Janegitz, T.B. Guerreiro, O.F. Filho, R.C. Faria and L.H.M.Junior *Electronalysis* 2 (2010) 1260
20. G.K. Dedzo, C.P.N. Njiki, and E. Ngameni, *Talanta* 99 (2012) 478.
21. X. Ye, Y. Gu, and C. Wang, C., *Sens. Actuators,* B 2012, vol.173, p. 537.
22. A. Farahi, M. Achak, L.E. Gaini, M.A. El Mhammedia, and M. Bakasse, *J. Food. Drug. Anal.* 23 (2015) 463.
23. N.C. Filho, F.D. L. Leite, E.R. Carvalho, E.C. Venâncio, C.M.P. Vaz, and L.H.C. Attoso, *J. Braz. Chem. Soc.* 18 (2007) 577.
24. H.C. Chang, T.J. Cheng, and R. J. Chen, *Electoanal.*10 (1998) 1275.
25. M.S.P.Shaffer, X. Fan, and A. H. Whindle, *Carbon* 36 *(*1998) 1603.
26. P. Gajendran, and R. Saraswathi, *J. Phys. Chem. C* 111 (2007) 11320.
27. V. Gupta, and N. Miura, *J. Power Sources.* 157(2006)616.
28. A. Walcarius, L. Lamberts, and E. G. Derouane, *Electroanal.* 7 (1995) 120.
29. R.F. Homer, G.C. Mees, and Tomlinson, *J. Sci. Food. Agri.* 11 (1960) 309.
30. P.M.S. Monk, C. Turner, and Akhtar, *Electrochim. Acta.* 44 (1999) 4817.
31. C.L.Bird, and A.T. Kuhn, *Chem. Soc. Rev*. 10 (1981*)* 49.
32. A.J. Bard Faulkner, Electrochemical Methods: Fundamentals and Applications, John Wiley, New York, 2001.
33. D.A. Skoog, F. J. Holler and Crouch, S.R., Instrumental Analysis, Cengage Learning, New

Delhi, 2007, pp. 135-151.
34. A. Farahi, M. Achakl, M.A. Gaini, El Mhammedi, and M. Bakasse,*Food Anal Methods*, 139 (2016) 9.
35. C. Kalinke, C., Mangrich,A.S., Marcolino-Junior, L.H., and Bergamini, M.F., *Electroanal.,* 28 (2016) 764.
36. A. Farahia, M. Achak, L. El Gaini, M.A. Mhammedia and M. Bakasse, *J. Food. Drug.Anal.*, 463 (2015) 23.
37. J. Gong, L. Wang, X. Miao and L. Zhang, *Electrochem. Comm*. 12 (2010) 1658.